mTORC1 Controls Murine Postprandial Hepatic Glycogen Synthesis Via *Ppp1r3b*

Kahealani Uehara[1,2,3], Won Dong Lee[4,5,6,], Megan Stefkovich[1], Dipsikha Biswas[7], Dominic Santoleri[1,2], Anna Garcia Whitlock[1,8], William Quinn III[1], Talia Coopersmith[1], Kate Townsend Creasy[1,9,10], Daniel J. Rader[1,9], Kei Sakamoto[7], Joshua D. Rabinowitz[4,5,6,11], Paul M. Titchenell[1,3]

[1]Institute for Diabetes, Obesity, and Metabolism, [2]Biochemistry and Molecular Biophysics Graduate Group, [3]Department of Physiology, Perelman School of Medicine, University of Pennsylvania, Philadelphia, Pennsylvania 19104, USA, [4]Lewis Sigler Institute for Integrative Genomics, [5]Department of Chemistry, [6]Ludwig Institute for Cancer Research, Princeton Branch, Princeton, NJ, USA, [7]Novo Nordisk Foundation Center for Basic Metabolic Research, University of Copenhagen, Copenhagen 2200, Denmark, [8]Department of Surgery, [9]Department of Medicine, Division of Translational Medicine and Human Genetics, [10]Department of Biobehavioral Health Sciences, School of Nursing, University of Pennsylvania, Philadelphia, Pennsylvania 19104, USA, [11]Department of Molecular Biology, Princeton University, Princeton, NJ, USA.

*Address correspondence:
Paul M. Titchenell, Ph.D.
3400 Civic Center Blvd.
Philadelphia, PA 19104
ptitc@pennmedicine.upenn.edu

KEY WORDS: glucose homeostasis, glycemia, glycogen storage disease, glycogen synthase

CONFLICTS OF INTEREST

D.J.R. owns equity in Alnylam and Verve Therapeutics. J.D.R. is a co-founder, stockholder, and director of Raze Therapeutics and Farber Partners; and an advisor and stockholder in Faeth Therapeutics, Empress Therapeutics, Bantam Pharmaceuticals, Colorado Research Partners, Rafael Pharmaceuticals, and L.E.A.F. Pharmaceuticals. None of these have any direct relationship to the manuscript.

ABSTRACT

In response to a meal, insulin drives hepatic glycogen synthesis to help regulate systemic glucose homeostasis. The mechanistic target of rapamycin complex 1 (mTORC1) is a well-established insulin target and contributes to the postprandial control of liver lipid metabolism, autophagy, and protein synthesis. However, its role in hepatic glucose metabolism is less understood. Here, we used metabolomics, isotope tracing, and mouse genetics to define a role for liver mTORC1 signaling in the control of postprandial glycolytic intermediates and glycogen deposition. We show that mTORC1 is required for glycogen synthase activity and glycogenesis. Mechanistically, hepatic mTORC1 activity promotes the feeding-dependent induction of *Ppp1r3b*, a gene encoding a phosphatase important for glycogen synthase activity whose polymorphisms are linked to human diabetes. Re-expression of *Ppp1r3b* in livers lacking mTORC1 signaling enhances glycogen synthase activity and restores postprandial glycogen content. mTORC1-dependent transcriptional control of *Ppp1r3b* is facilitated by FOXO1, a well characterized transcriptional regulator involved in the hepatic response to nutrient intake. Collectively, we identify a role for mTORC1 signaling in the transcriptional regulation of *Ppp1r3b* and the subsequent induction of postprandial hepatic glycogen synthesis.

INTRODUCTION

The liver is a central regulator of systemic glucose metabolism. Dysregulation of postprandial hepatic glucose metabolism contributes to the development of metabolic disorders, such as insulin resistance and type II diabetes (1). During periods of fasting, the liver breaks down glycogen stores via glycogenolysis to produce glucose and maintain circulating blood glucose levels (2,3). Upon feeding, blood glucose rises, causing an increase in insulin secretion from the pancreas, which drives anabolic metabolism in insulin-responsive tissues such as the liver, skeletal muscle, and adipose tissue.

In the postprandial liver, glucose is taken up and stored as glycogen, through a process called glycogenesis. Glycogen is synthesized from two pathways: (I) the direct pathway via glucose phosphorylation via glucokinase (GCK), the main hexokinase of the liver, and (II) the indirect pathway, in which gluconeogenic substrates fuel the generation of glycogen precursors. Overall, glycogenesis is driven by glucose-6-phosphate (G6P), and its conversion to glucose-1-phosphate (G1P) by phosphoglucomutase (4,5). G1P then reacts with uridine triphosphate (UTP) to generate uridine diphosphate glucose (UDP-glucose) via UDP-glucose pyrophosphorylase (UGP) (6). UDP-glucose is transferred to glycogen branches via glycogen synthase (GS), contributing to glycogen stores. A feedforward mechanism exists whereby G6P allosterically activates GS to stimulate glycogenesis (7-9). Additionally, phosphorylation of GS via glycogen synthase kinase 3 (GSK3) inhibits GS enzymatic activity and its dephosphorylation via protein phosphatase 1 (PP1) leads to GS activation (10,11). Glycogen storage is antagonized by glycogen phosphorylase (GP), the enzyme required for the phosphorylation of glycogen branches to generate and release G1P (12,13). PP1-mediated dephosphorylation of GP renders the enzyme inactive (10). Defects in the key enzymes involved in glycogen synthesis and breakdown underpin a variety of glycogen storage diseases (GSD) (14).

Furthermore, deficiency in the enzymes regulating GS and GP activities, namely PP1, associate with abnormal glycogen content (15).

Protein phosphatase 1 regulatory subunit 3B (PPP1R3B) is a feeding-induced, glycogen-targeting subunit of PP1 required for GS dephosphorylation and thus glycogenesis in the liver (16-19). Whole-body and liver-specific deletion of *Ppp1r3b* in mice prevents postprandial hepatic glycogen storage (16,17). Hepatic overexpression of *Ppp1r3b* in mice enhances glycogen storage, highlighting the importance of *Ppp1r3b* expression for glycogen maintenance (16,17,19). Notably, the Meta-Analyses of Glucose- and Insulin-related traits consortium (MAGIC) identified variants near the *PPP1R3B* locus that are associated with fasting insulin and fasting glucose (20,21). Given its importance in regulating postprandial glycogen storage and that genetic variations of *PPP1R3B* are associated with glycemic traits, *PPP1R3B* remains a gene of interest for T2D. However, the upstream signals controlling the regulation of *PPP1R3B* remain ill-defined.

Hepatic insulin action is critical for postprandial glycogen synthesis and the suppression of glucose production. Under conditions of insulin resistance, insulin fails to stimulate postprandial glycogen synthesis and suppress glucose production contributing to hyperglycemia (22). Insulin acts through the PI3K/AKT axis to stimulate glucose uptake and inhibit hepatic glucose production. Insulin action through AKT is required for stimulation of glycogenesis and inhibition of gluconeogenesis, through which glycogen synthase kinase 3 (GSK3) and forkhead box O (FOXO) transcription factors are involved, respectively. Interestingly, although downstream of AKT, the mechanistic target of rapamycin complex 1 (mTORC1) has not been previously demonstrated to contribute to hepatic glucose control. Several published reports show an important role for mTORC1 in liver biology including effects on protein synthesis, cell growth, and lipid synthesis and secretion (23). However, there is a dearth of information for mTORC1's

involvement in liver glucose metabolism. Long-term treatment of rapamycin in canines with glycogen storage disease IIIa (GSDIIIa), an autosomal disorder caused by a defect in glycogen debranching enzyme, reduces liver glycogen levels (24). In a separate study using immortalized hepatocytes (HepG2), insulin-mediated GS activation is blunted in response to rapamycin treatment (25). On the other hand, activation of mTORC1 via deletion of tuberous sclerosis 2 (TSC2), a negative regulator of mTORC1, caused an increase in intracellular glycogen content in MEFs (26). These data suggest that mTORC1 may promote glycogen storage; however, the underlying mechanisms are not known.

In this study, we demonstrate a requirement for hepatic mTORC1 signaling on glycolytic intermediates and postprandial hepatic glucose disposal via mTORC1-dependent control of glycogen synthase activity. First, we performed metabolomics in an acute liver-specific model of mTORC1 inhibition (referred to here as L-Raptor-KO) to identify changes in glycolytic metabolites dependent on mTORC1. Using ^{13}C-glucose tracing, we find that mTORC1 activity is required for feeding-induced glycogen synthesis. Mechanistically, we show that mTORC1 is required for the postprandial induction of *Ppp1r3b* mRNA expression and demonstrate that re-expression of *Ppp1r3b* in an mTORC1-null liver is sufficient to restore GS activity and feeding-induced hepatic glycogen synthesis. The mTORC1-dependent transcriptional regulation of *Ppp1r3b* is due, in part, to FOXO retention in the nucleus, rendering constitutive repression of *Ppp1r3b* and *Gck* transcripts. Collectively, data presented here describe a n mechanism for mTORC1 in the control of postprandial hepatic glucose storage and glycogen synthase activity.

RESULTS

Postprandial metabolomics reveal increased glycogen precursors in the absence of mTORC1 activity

In response to feeding and elevated systemic insulin levels, the liver rapidly shifts from a state of catabolism to anabolism. Our lab and others have focused on defining the global transcriptional response to nutrient intake (27). However, the acute changes in liver metabolites that occur with feeding are less defined. To understand how the liver metabolome changes in response to feeding, 16-hour fasted and four-hour refed murine livers were subjected to metabolomic analysis (Figure 1A, B). Of the 739 metabolites identified, 163 metabolites were differentially regulated (FC>2, or FC<-2, $p<0.01$) (Figure 1A, B). With respect to glucose metabolism, while G6P and phosphoenolpyruvate (PEP) increased, fructose-1,6-bisphosphate (FBP), glycerol-3-phosphate (G3P), and UDP-glucose decreased, with the strongest change in UDP-glucose (Figure 1C). G6P is analytically indistinguishable from other isomers in the liquid chromatography methods used, but it is the most abundant hexose phosphate, hence, we refer to this hexose phosphate as G6P.

Given that mTORC1 is a critical feeding-regulated kinase in hepatocytes (23), we generated mice lacking mTORC1 specially in hepatocytes from adult mice, to define mTORC1's role in the postprandial response. To do so, *Rptor*$^{loxP/loxP}$ mice were injected with a liver-specific adeno-associated virus (AAV), serotype 8, carrying GFP (Control) or Cre recombinase (L-Raptor-KO). Raptor is an essential subunit of the mTORC1 complex and deletion leads to complete loss of mTORC1 activity without affecting mTORC2 (28). Two weeks post-AAV injections, Raptor mRNA (Supplemental Figure 1A) and protein (Figure 1D) were reduced in L-Raptor-KO, and phosphorylation of the canonical mTORC1 downstream target ribosomal protein S6 decreased (Figure 1D). Metabolomic analysis of four hour-refed control and L-Raptor-KO livers revealed that out of the total 739 metabolites screened, 136 metabolites were upregulated (FC>2) in the

absence of mTORC1 signaling (Supplemental Figure 1B,C). Notably, a general decrease in glycolysis-related metabolites downstream of G6P including fructose 1,6-bisphosphate, glycerol 3-phosphate, and PEP was noted (Figure 1E). Surprisingly, there was an increase in the more proximal glycolytic metabolites including the glycogen precursors, UDP-glucose and G6P ($p=0.051$) (Figure 1E).

One explanation for the increased levels of UDP-glucose observed in refed L-Raptor-KO mice would be impaired consumption by glycogen synthesis. Accordingly, the levels of postprandial glycogen content were determined following loss of mTORC1 signaling. Postprandial liver glycogen content was significantly decreased in mTORC1-deficient livers, evidence by both an enzymatic assay and Periodic Acid Schiff (PAS) staining (Figure 1F, G). The reduced glycogen content in L-Raptor-KO livers is consistent with lower liver wet weights (Supplemental Figure 1D). Taken together, these data indicate that liver mTORC1 signaling is required for proper liver glycogen storage in the postprandial state.

mTORC1 is required for hepatic glycogen synthesis

Based on the increased G6P and UDP-glucose levels in L-Raptor-KO livers, as well as decreased hepatic glycogen (Figure 1E, F), we next investigated whether this was due to increased direct contribution of glucose to the G6P and UDP-glucose pools. mTORC1 signaling is required, but not sufficient, for lipogenic gene induction through activation of the transcription factor sterol regulatory binding protein 1c (SREBP1c) (29,30). One of the downstream targets of SREBP1c is glucokinase (GCK), the main hexokinase and glucose sensor in the liver (5). Previous studies have highlighted the importance for insulin signaling and SREBP1c processing in *Gck* mRNA regulation (Figure 2A) (31,32). Indeed, in mTORC1-deficient livers, a loss of mRNA expression of *Gck* in response to feeding was observed (Figure 2B). Despite this reduction in mRNA, there is only a modest reduction in GCK protein in L-Raptor-KO livers,

suggesting there is a distinction between mRNA regulation and protein regulation of GCK by mTORC1 (Figure 2C).

Next, ^{13}C-glucose labeling was performed to determine how mTORC1 controls postprandial glycogen accumulation. Overnight fasted control and L-Raptor-KO mice were administered an oral gavage with 2g/kg [U-^{13}C]glucose and the labeling of glycolytic metabolites and glycogen 30 minutes post-gavage was determined. Consistent with the findings from the steady-state metabolomics, L-Raptor-KO livers contained increased pool sizes of hexose phosphate and UDP-glucose (Figure 2D, 2E and Figure 1E), independent of changes plasma glucose labeling differences (Supplemental Figure 2A, B). However, there were no differences in isotope labeling of hexose phosphate, including M+6, implying that GCK protein is still functional in the absence of mTORC1 signaling (Figure 2C, 2D, Supplemental Figure 2C). Interestingly, an increase in the pool size of isotopomers (M+1…M+6) of UDP-glucose was detected in L-Raptor-KO livers consistent with buildup of glucose-derived carbons in UDP-glucose in L-Raptor-KO mice (Figure 2E, Supplemental Figure 2D). Consistent with impaired use of UDP-glucose to make glycogen, the enrichment of liver glycogen from circulating ^{13}C-glucose was significantly reduced in L-Raptor-KO livers (Figure 2F). Altogether, these data demonstrate that mTORC1 is required for hepatic glycogen synthesis from glucose, and this is independent of alterations in GCK activity.

mTORC1 controls glycogenesis through regulation of GS activity

Phosphorylation of GS renders the enzyme inactive, whereas dephosphorylation activates GS and promotes glycogenesis. Glycogen synthase kinase 3 (GSK3) phosphorylates and negatively regulates GS. Canonically, insulin stimulates the phosphorylation of GSK3 to inhibit its catalytic function, thereby preventing GS phosphorylation and inhibition, thus promoting glycogen synthesis. In L-Raptor-KO livers, GSK3 phosphorylation levels were increased in the refed state, which suggest that GSK3 is likely not involved in the downstream of mTORC1

regulating glycogenesis (Figure 3A). These findings are associated with increased phospho-AKT signal in L-Raptor KO mice due to relief of negative feedback inhibition by mTORC1 to proximal insulin signaling (Figure 2C). In addition, the levels of mRNA expression of *G6pc*, the phosphatase that converts G6P to glucose, and *Gys2*, the gene encoding the liver GS isoform, were no different between control and L-Raptor-KO mice (Figure 3B, C). Modest increases in *Pygl,* the gene encoding the liver GP isoform, were observed (Figure 3D). We measured GS activity and observed a significant blunting in the feeding induction of GS in the L-Raptor-KO livers compared to control animals (Figure 3E). These data suggest that mTORC1 controls postprandial hepatic glycogen synthesis in part via the regulation of GS activity, independent of increased G6P levels, a well-defined allosteric activator of GS (8).

Restoration of Ppp1r3b in L-Raptor-KO livers promotes GS activity and glycogen storage

As mentioned previously, GS activity is regulated by phosphorylation, of which PP1 family of phosphatases are an essential component in modulating glycogen levels. PPP1R3B, also known as G_L, is an essential regulatory subunit of PP1 complex, and genetic variations near the *PPP1R3B* locus are associated with fasting glucose and insulin (20). *Ppp1r3b* mRNA is induced upon feeding (17), and we find that this upregulation is dependent upon hepatic mTORC1 signaling (Figure 4A). These data suggest that mTORC1 regulates postprandial glycogen deposition via *Ppp1r3b* expression.

To test the sufficiency of *Ppp1r3b* in mediating the effects of mTORC1 on hepatic glycogen content, mice were co-injected with AAV8-TBG-Ppp1r3b along with AAV8-TBG-Cre, to generate a mouse re-expressing *Ppp1r3b* in Raptor-deficient hepatocytes (L-Raptor-KO + Ppp1r3b) (Figure 4B). Co-injection of AAV-Ppp1r3b and AAV-Cre resulted in deletion of *Rptor* gene and a functional decrease in mTORC1 signaling (Supplemental Figure 3A). This co-injection strategy led to increased *Ppp1r3b* mRNA levels; albeit not to the same extent as control mice

(Supplemental Figure 3A). The partial re-expression of *Ppp1r3b* in L-Raptor-KO resulted in a modest decrease in phosphorylation of glycogen synthase (p-GS) at Serine-641 compared to L-Raptor-KO alone, suggesting an increase in GS activity and glycogen synthesis (Figure 4C). This degree of an effect of AAV-PPP1R3B re-expression on Serine-641 are similar to changes reported previously (16). Notably, *PPP1r3b* re-expression correlated with an increase in glycogen synthase activity (~2 fold vs L-Raptor-KO) that was indistinguishable from control mice (Figure 4D). Moreover, PPP1R3B expression increased hepatic glycogen levels significantly in the mice lacking hepatic mTORC1 signaling (Figure 4E). Physiologically, the changes in glycogen content influenced systemic glycemia as food removal induced a hypoglycemic state within four hours in L-Raptor-KO mice, which was completely normalized by *Ppp1r3b* re-expression (Figure 4F). Of note, expression of *Ppp1r3b* did not alter mRNA expression of *Gck* and *G6pc* (Supplemental Figure 3B). Overall, restoring *Ppp1r3b* in mTORC1-ablated livers improved postprandial GS activity and enhanced hepatic glycogen storage leading to maintenance of fasting glycemia.

Exogenous SREBP1c expression fails to restore hepatic glycogen in L-Raptor-KO mice

To determine which transcription factors may mediate *Ppp1r3b* expression downstream of mTORC1, the canonical fasting/feeding transcription factors were profiled. Carbohydrate responsive element-binding protein (ChREBP) is a transcription factor involved in DNL which is, as its name suggests, responsive to glucose and other carbohydrates (33). ChREBPβ isoform (gene name *Mlxipl*, but referred to here as *ChrebpB*) mRNA expression was increased in L-Raptor-KO livers (Supplemental Figure 4A) and this expression corresponded with an induction in liver pyruvate kinase (*Pklr),* a transcriptional target of ChREBPβ, with no significant changes in xylulose-5-phosphate (34) (Supplemental Figure 4B, C). Increased ChREBPβ activation is likely due to increased G6P levels (Figure 1E, 2D), but would suggest that ChREBPβ acts as a

transcriptional repressor of *Ppp1r3b*. Since ChREBPβ is classically considered a transcriptional activator of glycolytic and lipogenic genes, attention was directed to other feeding-regulated transcription factors.

Srebp1c is induced with refeeding and its expression was significantly blunted in the refed mTORC1 deficient liver, as reported previously (Figure 2A) (30,35). Therefore, published cistromic and transcriptomic data were analyzed to determine if SREBP1c may act as transcription factor involved in *Ppp1r3b* expression. HA-nSREBP1c CHIP-Seq reveals SREBP1c binding near the transcription start site (TSS) of *Ppp1r3b* (36) (Supplemental Figure 5A). Furthermore, global run-on sequencing (GRO-seq) data were examined to explore active sites of enhancers (27). Interestingly, an enhancer RNA (eRNA) in proximity of the *Ppp1r3b* gene colocalized with *Srebp1c* binding (Supplemental Figure 5A). These data suggest that *Srebp1c* may regulate the expression of *Ppp1r3b* postprandially. To test this, an AAV transcribing the nuclear form of SREBP1c (nSREBP1c), rendering the protein constitutively active, was co-injected with either AAV-GFP or CRE to generate control or overexpress nSREBP1c in L-Raptor-KO mice. Two weeks post AAV injection, nSREBP1 increased lipogenic genes, *Fasn* and *Acaca,* but had no effect on *Gck* (Supplemental Figure 5B). Previous studies employing this AAV-nSREBP1c virus at the same dosage have validated its functional ability to restore DNL (36,37). Re-expression of *nSrebp1c*, however, did not restore *Ppp1r3b* mRNA expression, nor did it restore postprandial hepatic glycogen content in the absence of liver mTORC1 (Supplemental Figure 5C, D). Collectively, these data suggest that mTORC1 controls the postprandial induction of *Ppp1r3b* and glycogen content in a mTORC1-dependent, SREBP1c-independent manner.

mTORC1 activity is required for AKT-mediated inhibition of FOXO1 in the control of Ppp1r3b expression independent of Gck

Since both SREBP1c and ChREBPβ were unlikely to be responsible for the transcriptional control of *Ppp1r3b*, our focus shifted to other feeding-regulated transcription factors implicated in glycemic control. Downstream of AKT, FOXO transcription factors are critical regulators of hepatic glucose production. During periods of fasting, FOXO proteins localize to the nucleus where they promote transcription of gluconeogenic genes while recruiting co-repressors to repress transcription of glucose utilization genes such as *Gck* (38). Upon feeding, AKT is activated and directly phosphorylates FOXO, excluding it from the nucleus, inhibiting its transcriptional regulatory functions. Analyzing our published GRO-Seq dataset alongside a publicly available FOXO1 ChIP-seq dataset revealed FOXO binding occurs near an enhancer in proximity of *Ppp1r3b* (Figure 5A). FOXO1 binding is also identified at eRNAs localized near two canonical FOXO targets, insulin-like growth factor binding protein 1 (*Igfbp1)* and glucokinase (*Gck),* providing evidence that this ChIP-seq reliably detected FOXO binding as a transcriptional activator and repressor, respectively (Figure 5B,C).

Although the FOXO1-regulated gene, *Gck,* mRNA is blunted in L-Raptor-KO (Figure 2B), we next tested whether *Igfbp1* mRNA expression was altered in the absence of mTORC1 activity as an additional readout of FOXO1 transcriptional activity. Notably, *Igfbp1* is significantly upregulated in L-Raptor-KO (Figure 5D), confirming increased FOXO activity. Nuclear enrichment of control and L-Raptor-KO livers revealed strong nuclear retention of FOXO1, despite increased AKT activity (Figure 5E). To determine if FOXO1 is sufficient to repress *Ppp1r3b*, we utilized a transgenic mouse model harboring a mutant FOXO1 with alanine substituting serine at the three AKT-mediated phosphorylation sites, leading to constitutive retention of FOXO1 in the nucleus ($FOXO^{AAA}$) (39). To induce expression of the nuclear FOXOAAA mutant specifically in hepatocytes, $FOXO^{AAA}$ were injected with AAV8-TBG-CRE (L-

FOXOAAA) or AAV8-TBG-GFP (Control) in 8–10-week-old mice and harvested livers two weeks post-AAV injection. As predicted, constitutive FOXO1 activation in L-FOXOAAA mice yields an induction in *Igfbp1* and a repression of *Gck* (Figure 6A). Notably, increased FOXO1 activity was sufficient to suppress *Ppp1r3b* and result in a significant blunting of postprandial hepatic glycogen content (Figure 6B,C). Consistent with previous reports, these data indicate that mTORC1 activity is required for nuclear exclusion of AKT-mediated phosphorylated FOXO1, (40), and inhibition of FOXO is required for induction of *Ppp1r3b* and hepatic glycogen synthesis (Figure 6D).

Since GCK activity is also suppressed following activation of FOXO1, we next determined if GCK is required for feeding-induced *Ppp1r3b* expression. To do so, we used a mouse model lacking GCK in hepatocytes. $Gck^{loxP/loxP}$ mice were injected with AAV8-TBG-CRE (L-GCK-KO) or AAV8-TBG-GFP (Control) where detection of GCK protein and mRNA was lost (Figure 2C, Supplemental Figure 6A). In the absence of hepatic GCK, *Ppp1r3b* mRNA remains unchanged, revealing that GCK signaling is not required to induce *Ppp1r3b* (Supplemental Figure 6B). Collectively, these data indicate a requirement for mTORC1 in FOXO1 nuclear exclusion and inhibition and suggest that both AKT and mTORC1 activity are required but not sufficient to control hepatic FOXO1 activity and glycogen accumulation.

DISCUSSION

The data presented in this manuscript demonstrate a requirement for mTORC1 in postprandial glycogen synthesis. Here we demonstrate that mTORC1 controls the feeding induction of *Ppp1r3b* to regulate glycogen synthase activity and glycogenesis through inhibition of FOXO1. Furthermore, we identify differential changes in metabolite pools as the liver transitions from a nutrient-deprived to a nutrient-abundant feeding state. Taken together, these findings highlight an essential role for mTORC1 in hepatic glucose metabolism and highlights the importance of *Ppp1r3b* in glycogen homeostasis and transcriptional mechanisms governing its molecular regulation.

Deletion of the liver-specific isoform of glycogen synthase (*Gys2)* in mice results in an almost complete depletion of liver glycogen content (41). Additionally, human loss of function mutations that cause a deficiency in glycogen synthase, specifically GSD Type 0 (GSD0), have depleted glycogen stores in the liver (42). Taken together, glycogen synthase activity is an essential regulator of hepatic glycogen content. A potent regulator of GS activity is PP1, including the hepatic G_L subunit, PPP1R3B. As previously noted, genetic variations near the *PPP1R3B* locus are associated with fasting insulin and fasting glucose, as characterized in the MAGIC study (20). Although we detect modest changes in phospho-GS at Serine-641 that correspond with robust functional changes in GS activity, additional phosphorylation sites on GS such as Ser8 may also be regulated by this mTORC1-PPP1R3B axis (43). Therefore, it is critical to understand the postprandial mechanisms regulating *Ppp1r3b* expression and GS activity. In our manuscript, we add mechanistic insight into how nutrient intake regulates *Ppp1r3b* and GS activity contributing to postprandial glycogen synthesis.

Despite many studies using rapamycin as a pharmacological approach to inhibit mTORC1, many fail to report how rapamycin impacts glycogen levels in the liver. However, existing

evidence suggest that rapamycin treatment blunts GS activity and glycogen synthesis. In a canine model of GSDIIIa, rapamycin treatment downregulated total hepatic glycogen content (24). In skeletal muscle models, rapamycin treatment led to increased GS phosphorylation, consistent with decreased GS activity, and further blunting of insulin-stimulated glycogen synthesis (44,45). Long-term rapamycin use is linked to impaired glucose tolerance and insulin sensitivity in rodent models (46,47). Chronic administration of rapamycin also inhibits mTORC2-AKT making it difficult to isolate the specific effects of hepatic mTORC1 in the control of glycogen content (28) highlighting the importance of this study that specifically isolates the role of hepatic mTORC1 signaling on glycogen synthesis and glucose homeostasis.

Our data demonstrate the requirement of mTORC1 signaling for glycogen synthesis via acute liver-specific deletion of Raptor protein. Other data involving constitutive activation of mTORC1, via deletion of the negative regulator of mTORC1, TSC, support these findings. In *Tsc2* deficient MEFs, intracellular glycogen accumulated to higher levels above control cells, which was reversed with rapamycin treatment or Raptor knockdown (26). Human loss-of-function mutations in tuberous sclerosis complex (TSC), for example cardiac rhabdomyomas, present with excess glycogen deposition, correlating with increased mTORC1 activity (48,49). Similarly, in mice lacking TSC1 in ventricular myocytes, myocytes had unrestrained mTORC1 activity and accumulated glycogen (50). Collectively, data from TSC studies support mTORC1 activation promoting glycogenesis in cells other than hepatocytes. However, it is challenging to interpret data from TSC-deficient models, as constitutive activation negatively impacts AKT activity, in which AKT is required for postprandial hepatic glycogen storage (22,37,51,52). This is consistent with studies that show loss of TSC in hepatocytes decreases hepatic glycogen content which is likely due to the downregulation of AKT signaling which occurs in little as two-weeks following TSC deletion in adult liver (53,54). Collectively, these data indicate that mTORC1 is required but not sufficient to control hepatic glycogenesis.

Mechanistically, our data demonstrate the requirement for mTORC1 activity in the nuclear exclusion and inhibition of FOXO1 in the induction of *Ppp1r3b* and glycogen synthesis. Previous studies demonstrate nuclear accumulation of AKT-phosphorylated FOXO in the absence of mTORC1 activation (40). Furthermore, our data correspond with prior observations of hepatic glycogen accumulation following FOXO inhibition (55). These data illustrate the requirement for mTORC1 in the canonical AKT-dependent inhibition of FOXO proteins (Figure 6G) and that phosphorylation of FOXO1 via AKT is not sufficient to drive nuclear export in the absence of mTORC1. Understanding the complex molecular interplay between AKT and mTORC1 in the regulation of FOXO1 is critical to our understanding of hepatic metabolism and will be the focus of future studies.

In summary, we provide evidence for a feeding-dependent mechanism of GS regulation and glycogenesis through *Ppp1r3b* via the nutrient-sensing kinase, mTORC1. These data provide additional mechanistic insight into the molecular control of postprandial glucose metabolism and provide important physiological context to the molecular regulation of a type 2 diabetes gene, *Ppp1r3b*. Elucidating the postprandial mechanisms of glucose disposal is vital for our understanding of liver physiology in health and disease such as insulin resistance and type 2 diabetes.

METHODS

Sex as a biological variable. This study exclusively examined male mice, however we expect similar results in female mice, due to the well-established role of mTORC1 in hepatic metabolism.

Animal experiments. *Rptor*$^{loxp/loxp}$, *Gck*$^{oxp/loxp}$, *Foxo1*$^{loxp/loxp}$, and *Foxo1*^{AAA} (otherwise known as R26StopFlFoxo1^{AAA}) mice were backcrossed to the C57BL/6 background (39,52,56,57), housed, and bred under specific pathogen–free conditions in facilities at the University of Pennsylvania. For acute excision of liver-specific genes, mice were injected with adeno-associated virus (Vector Core, University of Pennsylvania) containing a liver-specific thyroxine binding globulin (TBG) promoter serotype 8 (AAV8-TBG) containing either GFP (AAV-GFP) or Cre (AAV-Cre) at a dosage of 1.0×10^{11} genome copies. AAV8-TBG-nSREBP1c virus was a kind gift from Dr. Mitchell Lazar (University of Pennsylvania). All mice were fed chow diet (LabDiet, #5010) unless specified otherwise. Control animals consist of pools of the appropriate floxed mice for each experiment *Rptor*$^{loxp/loxp}$, that were injected with AAV-GFP. Mice that were co-injected with AAV-Ppp1r3b or AAV-nSREBP1c and AAV-cre received 3.0×10^{11} and 1.0×10^{11} genome copies, respectively, for a total of 4.0×10^{11} genome copies in a singular injection. Consistently, control mice were injected with 4.0×10^{11} genome copies of AAV-GFP, and L-Raptor-KO mice were injected with 1.0×10^{11} and 3.0×10^{11} of AAV-Cre and AAV-GFP, respectively, for a total injection of 4.0×10^{11} genome copies. All experiments were performed in male mice.

Tissue metabolite extraction. Mice were euthanized by cervical dislocation. Tissues were quickly dissected and snap frozen in liquid nitrogen with a precooled clamp. Snap-frozen tissues were transferred to 2-mL round-bottom Eppendorf Safe-Lock tubes on dry ice. Samples were then ground into powder with a cryomill machine (21) for 30s at 25 Hz and maintained at a cold

temperature using liquid nitrogen. For every 20 mg tissue, 800μL −20 °C 40:40:20 (v/v/v) acetonitrile:methanol:water solution was added to the tube, vortexed for 10 s, and then centrifuged at 21,000 × g for 20 min at 4 °C. The supernatants were then transferred to plastic vials for LC-MS analysis. A procedure blank was generated identically without tissue and was used later to remove the background ions.

Plasma metabolite extraction. Plasma (2.5μL) was added to 60 μL −20 °C 25:25:10 (v/v/v) acetonitrile:methanol:water solution, vortexed for 10 s, and put on ice for at least 5 min. The resulting extract was centrifuged at 21,000 × g for 20 min at 4 °C and supernatant was transferred to tubes for LC-MS analysis. A procedure blank was generated identically without plasma, which was used later to remove the background ions.

Metabolite measurement by LC-MS. Metabolites were analyzed using a Vanquish Horizon UHPLC System (Thermo Scientific) coupled to an Orbitrap Exploris 480 mass spectrometer (Thermo Scientific). Waters XBridge BEH Amide XP Column [particle size, 2.5 μm; 150 mm (length) × 2.1 mm (i.d.)] was used for hydrophilic interaction chromatography (HILIC) separation. Column temperature was kept at 25 °C. Mobile phases A = 20 mM ammonium acetate and 22.5 mM ammonium hydroxide in 95:5 (v/v) water:acetonitrile (pH 9.45) and B = 100% acetonitrile were used for both ESI positive and negative modes. The linear gradient eluted from 90% B (0.0 to 2.0 min), 90% B to 75% B (2.0 to 3.0 min), 75% B (3.0 to 7.0 min), 75% B to 70% B (7.0 to 8.0 min), 70% B (8.0 to 9.0 min), 70% B to 50% B (9.0 to 10.0 min), 50% B (10.0 to 12.0 min), 50% B to 25% B (12.0 to 13.0 min), 25% B (13.0 to 14.0 min), 25% B to 0.5% B (14.0 to 16.0 min), 0.5% B (16.0 to 20.5 min), then stayed at 90% B for 4.5 min. The flow rate was 0.15 mL/min. The sample injection volume was 5 μL. ESI source parameters were set as follows: spray voltage, 3,200 V or −2,800 V, in positive or negative modes, respectively; sheath gas, 35 arb; aux gas, 10 arb; sweep gas, 0.5 arb; ion transfer tube temperature, 300 °C;

vaporizer temperature, 35 °C. LC–MS data acquisition was operated under a full-scan polarity switching mode for all samples. The full scan was set as orbitrap resolution, 120,000 at m/z 200; AGC target, 1e7; maximum injection time, 200 ms; scan range, 60 to 1,000 m/z.

Data analysis. LC-MS raw data files (.raw) were converted to mzXML format using ProteoWizard (version 3.0.20315). El-MAVEN (version 0.12.0) was used to generate a peak table containing m/z, retention time, and intensity for the peaks. Parameters for peak picking were the defaults except for the following: mass domain resolution, 5 ppm; time domain resolution, 10 scans; minimum intensity, 10,000; and minimum peak width, five scans. The resulting peak table was exported as a .csv file. Peak annotation of untargeted metabolomics data was performed using NetID with default parameters. For tracer experiments, isotope labeling was corrected for ^{13}C natural abundances using AccuCor package.

Immunoblots. Protein lysates were prepared from frozen livers in a modified RIPA buffer with Phosphatase Inhibitor Cocktails 2 and 3 (Sigma-Aldrich) and cOmplete Protease Inhibitor Cocktail (58), as described previously (29). The following antibodies were used for immunoblotting: p-AKT (CST #4060), AKT2 (CST #2964), p-S6 (CST #2215), S6 (CST #2217), HSP90 (CST #4874), GCK (Gift from Magnuson Lab), p-GS (CST #3891), p-GSK3β (CST #9336), Raptor (CST #2280), FOXO1 (CST #9454).

mRNA Isolation and Real-Time PCR. Total RNA was isolated from frozen livers using the RNeasy Plus kit (Qiagen). Complementary DNA was synthesized using Moloney murine leukemia virus (MulV) reverse transcriptase, and the relative expression of the genes of interest was quantified by real-time PCR using the SYBR Green dye-based assay.

Histology. Livers were fixed in 10% buffered formalin overnight, dehydrated in ethanol, paraffin-embedded and sectioned. Sections were stained with hematoxylin and eosin or Periodic acid-Schiff (PAS) staining.

Liver glycogen determination. Glycogen was extracted from 100 mg of liver in 6% perchloric acid by digesting the samples in KOH followed by digestion with amylo-glucosidase (Sigma Aldrich). Resulting free glycosyl units were assayed spectrophotometrically using a hexokinase-based glucose assay kit (Sigma Aldrich) and compared to the glucose levels in the samples prior to enzymatic digestion.

Glycogen synthase activity assay. Liver tissues were weighed and homogenized in 1:20 (wet) mass/ml ice cold lysis buffer (270 mM sucrose, 50 mM Tris-HCl (pH 7.5), 1 mM EDTA, 1 mM EGTA, 1% (v/v) Triton X-100, 20 mM glycerol-2-phosphate, 50 mM NaF, 5 mM Na4P2O7, 1 mM DTT, 0.1 mM PMSF, 1 mM benzamidine, 1 mg/mL microcystin-LR, 2 mg/mL leupeptin, and 2 mg/mL pepstatin A), followed by centrifugation at 3000g for 5min at 4 °C. Glycogen synthase activity in the liver lysates was determined as described previously (8). Briefly, clarified lysates were diluted to a concentration of 2.5 mg/ml with ice cold lysis buffer in a total volume of100 µL. 20 µL of the protein solution was added to 80 µL of the assay buffer (25 mM Tris-HCl (pH 7.8), 50 mM NaF, 5 mM EDTA, 10 mg/ml glycogen), 5.5 mM UDP-glucose, 12.5 m-m Na_2SO_4, 0.125% (v/v) β-mercaptoethanol and 0.05 mCi/mmol or 0.15 mCi/mmol D-[^{14}C]-UDP-glucose (American Radiolabelled Chemicals, Inc., ARC 0154) with or without 12.5 mM G6P. Note: 0.05 mCi/mmol D-[^{14}C]-UDP-glucose was used for the samples incubated in the presence of G6P and 0.15 mCi/mmol D-[^{14}C]-UDP-glucose was used for the samples incubated in the absence of G6P (due to very low basal glycogen synthase activity in the liver). The reaction mixtures were incubated for 30 min at 30 °C with mild agitation at 300 rpm. The reactions were stopped by spotting 90 µL of the reaction mix onto 2.5 cm × 2.5 cm squares of filter paper (Whatman 3MM)

which were immediately immersed in ice cold 66% ethanol and left to incubate with mild agitation for 20 min. The filter papers were washed thrice more in 66% ethanol for 20 min each and rinsed in acetone. The dried filters were subjected to scintillation counting.

Statistical analysis. Statistical analysis was performed using One-way ANOVAs when more than two groups were compared, 2-way ANOVAs when two conditions were analyzed, and unpaired two-tailed Students' t test when two groups were being assayed. All data were presented as mean ± SEM. * indicates p value < 0.05, ** indicates p value < 0.01, *** indicates p value < 0.001, **** indicates p value < 0.0001 vs. indicated genotype.

Study approval. Animal use followed all standard and guidelines of the Institutional Animal Care and Use Committee (IACUC) at the University of Pennsylvania.

Data availability. Data available in the "Supporting data values" XLS file

AUTHOR CONTRIBUTIONS

K.U. conceived the hypothesis, designed and performed experiments, analyzed data, and prepared the manuscript. W.D.L. provided technical assistance, contributed to experimental design, and analyzed data. W.J.Q. and D.S. designed and performed experiments and analyzed data. D.B. performed experiments and analyzed data. M.S., T.C., A.G.W., and M.G. provided technical assistance. K.T.C. and J.D.R. contributed conceptually to experimental design and data analysis. K.S. contributed to experimental design and analyzed data. D.J.R. provided virus and contributed to experimental design. P.M.T. conceived the hypothesis, designed and performed experiments, analyzed data, prepared the manuscript, and directed the project.

ACKNOWLEDGEMENTS

We thank Lan Cheng for her expert tissue processing and histology. We also acknowledge support from the Penn Vector Core, Penn Diabetes Research Center (P30-DK19525), and the Penn Center for Molecular Studies in Digestive and Liver Diseases (P30-DK050306). We thank Dr. Mitchell Lazar for their kind gift of the AAV-nSREBP1c. Lastly, a special thanks to all the members of the Titchenell lab for their thoughtful discussions on this project.

This work was supported by U.S. National Institutes of Health (NIH) grant R01-DK125497 (P.M.T.), UM1126194 (D.J.R, P.M.T), NIH NRSA F31-DK128876 (K.U.), NIH R01-DK114291 (K.T.C. and D.J.R.), NIH NRSA F32-DK127843 (W.D.L.), Novo Nordisk Foundation (20) NNF18CC0034900 (K.S.), and International Postdoctoral Fellowship by the Novo Nordisk Foundation Center for Basic Metabolic Research (D.B.), and Cox Research Institute.

REFERENCES

1. Santoleri D, Titchenell PM. Resolving the Paradox of Hepatic Insulin Resistance. *Cell Mol Gastroenterol Hepatol*. 2019;7(2):447-456. doi:10.1016/j.jcmgh.2018.10.016

2. Nordlie RC, Arion WJ. Evidence For The Common Identity Of Glucose 6-Phosphatase, Inorganic Pyrophosphatase, And Pyrophosphate-Glucose Phosphotransferase. *J Biol Chem*. Jun 1964;239:1680-5.

3. Pilkis SJ, et al. Hormonal regulation of hepatic gluconeogenesis and glycolysis. *Annu Rev Biochem*. 1988;57:755-83. doi:10.1146/annurev.bi.57.070188.003543

4. Adeva-Andany María M, et al. Liver glucose metabolism in humans. *Bioscience Reports*. 2016;36(6)doi:10.1042/bsr20160385

5. Matschinsky FM, Wilson DF. The Central Role of Glucokinase in Glucose Homeostasis: A Perspective 50 Years After Demonstrating the Presence of the Enzyme in Islets of Langerhans. *Front Physiol*. 2019;10:148. doi:10.3389/fphys.2019.00148

6. Stevens RA, Phelps CF. Studies on ligand binding to bovine liver uridine diphosphate glucose pyrophosphorylase. *Biochem J*. Oct 1 1976;159(1):65-70. doi:10.1042/bj1590065

7. Roach PJ, Larner J. Covalent phosphorylation in the regulation of glycogen synthase activity. *Molecular and Cellular Biochemistry*. 1977/05/01 1977;15(3):179-200. doi:10.1007/BF01734108

8. von Wilamowitz-Moellendorff A, et al. Glucose-6-phosphate-mediated activation of liver glycogen synthase plays a key role in hepatic glycogen synthesis. *Diabetes*. Dec 2013;62(12):4070-82. doi:10.2337/db13-0880

9. Bouskila M, et al. Allosteric regulation of glycogen synthase controls glycogen synthesis in muscle. *Cell Metab*. Nov 3 2010;12(5):456-66. doi:10.1016/j.cmet.2010.10.006

10. Cohen PT. Protein phosphatase 1--targeted in many directions. *J Cell Sci*. Jan 15 2002;115(Pt 2):241-56. doi:10.1242/jcs.115.2.241

11. McManus EJ, et al. Role that phosphorylation of GSK3 plays in insulin and Wnt signalling defined by knockin analysis. *Embo j*. Apr 20 2005;24(8):1571-83. doi:10.1038/sj.emboj.7600633

12. Maddaiah VT, Madsen NB. Kinetics of purified liver phosphorylase. *J Biol Chem*. Sep 10 1966;241(17):3873-81.

13. Stalmans W, Hers HG. The stimulation of liver phosphorylase b by AMP, fluoride and sulfate. A technical note on the specific determination of the a and b forms of liver glycogen phosphorylase. *Eur J Biochem*. Jun 1975;54(2):341-50. doi:10.1111/j.1432-1033.1975.tb04144.x

14. Ozen H. Glycogen storage diseases: new perspectives. *World J Gastroenterol*. May 14 2007;13(18):2541-53. doi:10.3748/wjg.v13.i18.2541

15. Newgard CB, et al. Organizing glucose disposal: emerging roles of the glycogen targeting subunits of protein phosphatase-1. *Diabetes*. Dec 2000;49(12):1967-77. doi:10.2337/diabetes.49.12.1967

16. Mehta MB, et al. Hepatic protein phosphatase 1 regulatory subunit 3B (Ppp1r3b) promotes hepatic glycogen synthesis and thereby regulates fasting energy homeostasis. *J Biol Chem*. Jun 23 2017;292(25):10444-10454. doi:10.1074/jbc.M116.766329

17. Stender S, et al. Relationship between genetic variation at PPP1R3B and levels of liver glycogen and triglyceride. *Hepatology*. Jun 2018;67(6):2182-2195. doi:10.1002/hep.29751

18. Doherty MJ, et al. Amino acid sequence and expression of the hepatic glycogen-binding (GL)-subunit of protein phosphatase-1. *FEBS Lett*. Nov 20 1995;375(3):294-8. doi:10.1016/0014-5793(95)01184-g

19. Creasy KT, et al. PPP1R3B is a metabolic switch that shifts hepatic energy storage from lipid to glycogen. *bioRxiv*. 2023:2023.03.04.529958. doi:10.1101/2023.03.04.529958

20. Manning AK, et al. A genome-wide approach accounting for body mass index identifies genetic variants influencing fasting glycemic traits and insulin resistance. *Nature Genetics*. 2012;44(6):659-669. doi:10.1038/ng.2274

21. Williamson A, et al. Genome-wide association study and functional characterization identifies candidate genes for insulin-stimulated glucose uptake. *Nature Genetics*. 2023/06/01 2023;55(6):973-983. doi:10.1038/s41588-023-01408-9

22. Wan M, et al. A noncanonical, GSK3-independent pathway controls postprandial hepatic glycogen deposition. *Cell Metab*. Jul 2 2013;18(1):99-105. doi:10.1016/j.cmet.2013.06.001

23. Ben-Sahra I, Manning BD. mTORC1 signaling and the metabolic control of cell growth. *Curr Opin Cell Biol*. Apr 2017;45:72-82. doi:10.1016/j.ceb.2017.02.012

24. Yi H, et al. Correction of glycogen storage disease type III with rapamycin in a canine model. *J Mol Med (Berl)*. Jun 2014;92(6):641-50. doi:10.1007/s00109-014-1127-4

25. Varma S, et al. Long-term effects of rapamycin treatment on insulin mediated phosphorylation of Akt/PKB and glycogen synthase activity. *Exp Cell Res*. Apr 1 2008;314(6):1281-91. doi:10.1016/j.yexcr.2007.12.019

26. Pal R, et al. Abnormal glycogen storage in tuberous sclerosis complex caused by impairment of mTORC1-dependent and -independent signaling pathways. *Proc Natl Acad Sci U S A*. Feb 19 2019;116(8):2977-2986. doi:10.1073/pnas.1812943116

27. Santoleri D, et al. Global-run on sequencing identifies Gm11967 as an Akt-dependent long noncoding RNA involved in insulin sensitivity. *iScience*. 2022;25(6):104410. doi:10.1016/j.isci.2022.104410

28. Lamming DW, et al. Rapamycin-Induced Insulin Resistance Is Mediated by mTORC2 Loss and Uncoupled from Longevity. *Science*. 2012;335(6076):1638-1643. doi:10.1126/science.1215135

29. Titchenell PM, et al. Direct Hepatocyte Insulin Signaling Is Required for Lipogenesis but Is Dispensable for the Suppression of Glucose Production. *Cell Metab*. Jun 14 2016;23(6):1154-1166. doi:10.1016/j.cmet.2016.04.022

30. Yecies JL, et al. Akt stimulates hepatic SREBP1c and lipogenesis through parallel mTORC1-dependent and independent pathways. *Cell Metab*. Jul 6 2011;14(1):21-32. doi:10.1016/j.cmet.2011.06.002

31. Foretz M, et al. Sterol regulatory element binding protein-1c is a major mediator of insulin action on the hepatic expression of glucokinase and lipogenesis-related genes. *Proc Natl Acad Sci U S A*. Oct 26 1999;96(22):12737-42. doi:10.1073/pnas.96.22.12737

32. Foretz M, et al. ADD1/SREBP-1c is required in the activation of hepatic lipogenic gene expression by glucose. *Mol Cell Biol*. May 1999;19(5):3760-8. doi:10.1128/mcb.19.5.3760

33. Li MV, et al. Glucose-dependent transcriptional regulation by an evolutionarily conserved glucose-sensing module. *Diabetes*. May 2006;55(5):1179-89. doi:10.2337/db05-0822

34. Kabashima T, et al. Xylulose 5-phosphate mediates glucose-induced lipogenesis by xylulose 5-phosphate-activated protein phosphatase in rat liver. *Proc Natl Acad Sci U S A*. Apr 29 2003;100(9):5107-12. doi:10.1073/pnas.0730817100

35. Owen JL, et al. Insulin stimulation of SREBP-1c processing in transgenic rat hepatocytes requires p70 S6-kinase. *Proc Natl Acad Sci U S A*. Oct 2 2012;109(40):16184-9. doi:10.1073/pnas.1213343109

36. Papazyan R, et al. Physiological Suppression of Lipotoxic Liver Damage by Complementary Actions of HDAC3 and SCAP/SREBP. *Cell Metab*. Dec 13 2016;24(6):863-874. doi:10.1016/j.cmet.2016.10.012

37. Uehara K, et al. Activation of Liver mTORC1 Protects Against NASH via Dual Regulation of VLDL-TAG Secretion and De Novo Lipogenesis. *Cell Mol Gastroenterol Hepatol*. 2022;13(6):1625-1647. doi:10.1016/j.jcmgh.2022.02.015

625 38. Langlet F, et al. Selective Inhibition of FOXO1 Activator/Repressor Balance Modulates
626 Hepatic Glucose Handling. *Cell*. 2017;171(4):824-835.e18. doi:10.1016/j.cell.2017.09.045
627 39. Ouyang W, et al. Novel Foxo1-dependent transcriptional programs control T(reg) cell
628 function. *Nature*. Nov 22 2012;491(7425):554-9. doi:10.1038/nature11581
629 40. Mori S, et al. The mTOR pathway controls cell proliferation by regulating the FoxO3a
630 transcription factor via SGK1 kinase. *PLoS One*. 2014;9(2):e88891.
631 doi:10.1371/journal.pone.0088891
632 41. Irimia JM, et al. Impaired glucose tolerance and predisposition to the fasted state in liver
633 glycogen synthase knock-out mice. *J Biol Chem*. Apr 23 2010;285(17):12851-61.
634 doi:10.1074/jbc.M110.106534
635 42. Orho M, et al. Mutations in the liver glycogen synthase gene in children with
636 hypoglycemia due to glycogen storage disease type 0. *J Clin Invest*. Aug 1 1998;102(3):507-15.
637 doi:10.1172/jci2890
638 43. Ros S, et al. Control of liver glycogen synthase activity and intracellular distribution by
639 phosphorylation. *J Biol Chem*. Mar 6 2009;284(10):6370-8. doi:10.1074/jbc.M808576200
640 44. Ashe KM, et al. Inhibition of glycogen biosynthesis via mTORC1 suppression as an
641 adjunct therapy for Pompe disease. *Mol Genet Metab*. Aug 2010;100(4):309-15.
642 doi:10.1016/j.ymgme.2010.05.001
643 45. Sipula IJ, et al. Rapamycin-mediated inhibition of mammalian target of rapamycin in
644 skeletal muscle cells reduces glucose utilization and increases fatty acid oxidation. *Metabolism*.
645 Dec 2006;55(12):1637-44. doi:10.1016/j.metabol.2006.08.002
646 46. Cunningham JT, et al. mTOR controls mitochondrial oxidative function through a YY1–
647 PGC-1α transcriptional complex. *Nature*. 2007;450(7170):736-740. doi:10.1038/nature06322
648 47. Fraenkel M, et al. mTOR inhibition by rapamycin prevents beta-cell adaptation to
649 hyperglycemia and exacerbates the metabolic state in type 2 diabetes. *Diabetes*. Apr
650 2008;57(4):945-57. doi:10.2337/db07-0922

48. Fenoglio JJ, Jr., et al. Cardiac rhabdomyoma: a clinicopathologic and electron microscopic study. *Am J Cardiol*. Aug 1976;38(2):241-51. doi:10.1016/0002-9149(76)90157-0

49. Hinton RB, et al. Cardiovascular manifestations of tuberous sclerosis complex and summary of the revised diagnostic criteria and surveillance and management recommendations from the International Tuberous Sclerosis Consensus Group. *J Am Heart Assoc*. Nov 25 2014;3(6):e001493. doi:10.1161/jaha.114.001493

50. Meikle L, et al. A mouse model of cardiac rhabdomyoma generated by loss of Tsc1 in ventricular myocytes. *Hum Mol Genet*. Feb 1 2005;14(3):429-35. doi:10.1093/hmg/ddi039

51. Quinn WJ, 3rd, et al. mTORC1 stimulates phosphatidylcholine synthesis to promote triglyceride secretion. *J Clin Invest*. Nov 1 2017;127(11):4207-4215. doi:10.1172/JCI96036

52. Lu M, et al. Insulin regulates liver metabolism in vivo in the absence of hepatic Akt and Foxo1. *Nat Med*. Feb 19 2012;18(3):388-95. doi:10.1038/nm.2686

53. Uehara K, et al. Activation of Liver mTORC1 Protects Against NASH via Dual Regulation of VLDL-TAG Secretion and De Novo Lipogenesis. *Cellular and Molecular Gastroenterology and Hepatology*. 2022;doi:10.1016/J.JCMGH.2022.02.015

54. Kucejova B, et al. Hepatic mTORC1 Opposes Impaired Insulin Action to Control Mitochondrial Metabolism in Obesity. *Cell Rep*. Jul 12 2016;16(2):508-519. doi:10.1016/j.celrep.2016.06.006

55. Haeusler RA, et al. Integrated control of hepatic lipogenesis versus glucose production requires FoxO transcription factors. *Nat Commun*. Oct 13 2014;5:5190. doi:10.1038/ncomms6190

56. Sengupta S, et al. mTORC1 controls fasting-induced ketogenesis and its modulation by ageing. *Nature*. Dec 23 2010;468(7327):1100-4. doi:10.1038/nature09584

57. Postic C, et al. Dual Roles for Glucokinase in Glucose Homeostasis as Determined by Liver and Pancreatic β Cell-specific Gene Knock-outs Using Cre Recombinase. *Journal of Biological Chemistry*. 1999;274(1):305-315. doi:10.1074/jbc.274.1.305

58. Commerford SR, et al. Dissection of the insulin-sensitizing effect of liver X receptor ligands. *Mol Endocrinol*. Dec 2007;21(12):3002-12. doi:10.1210/me.2007-0156

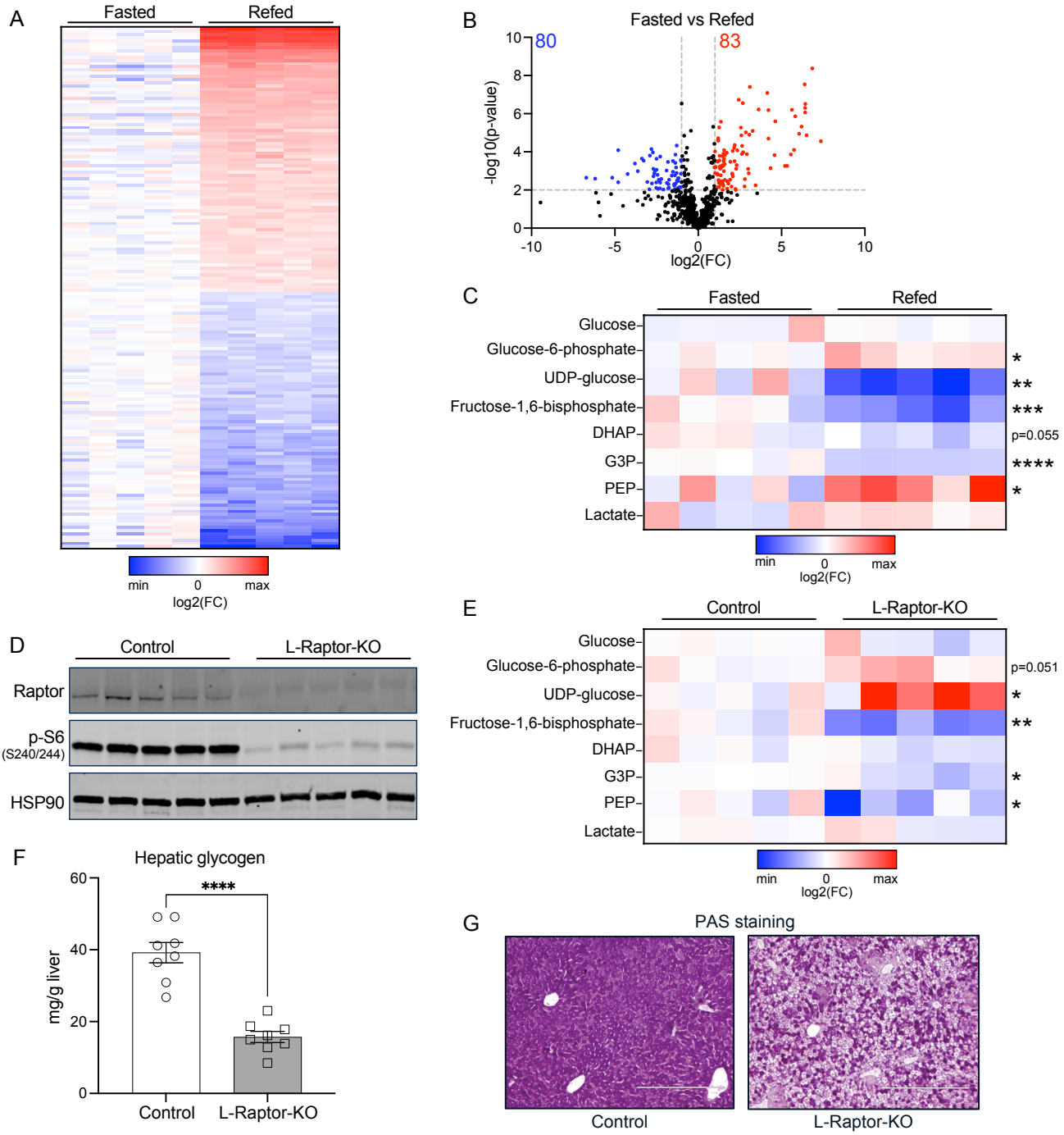

Figure 1: Postprandial metabolomics reveal increased glycogen precursors in the absence of mTORC1 activity
(A-C) 10-12 week-old mice were fasted for 16 hours (Fasted) then given food for 4 hours (Refed). (A) Heat map of differential metabolite abundance shown as log2(fold change) compared to fasted livers. (B) Volcano plot showing -log10(p-value vs. fasted) on y-axis and log2(fold change vs fasted) on x-axis. Blue dots represent log2(FC)<-2, p<0.01. Red dots represent log2(FC)>2, and p<0.01. (C) Selected glucose metabolites relative abundance. (D-G) 10-12 week old *Rptor*$^{loxP/loxP}$ mice were injected with AAV8-TBG-Cre (L-Raptor-KO) or AAV8-TBG-GFP (Control). Two weeks after injection, mice were fasted overnight, then refed chow for 4 hours before sacrifice. (D) Immunoblot demonstrating loss of Raptor protein and inhibition of mTORC1 signaling. (E) Heat map of selected glucose metabolite relative abundance shown as log2(fold change) compared to control fed livers. (F) Hepatic glycogen in fed livers. Data shown as mean +/- SEM. (G) Periodic acid-Schiff staining for glycogen (pink). *p<0.05, **p<0.0t1, ***p<0.001, ****p<0.0001 vs control via students t-test. Red indicates higher metabolite abundance.

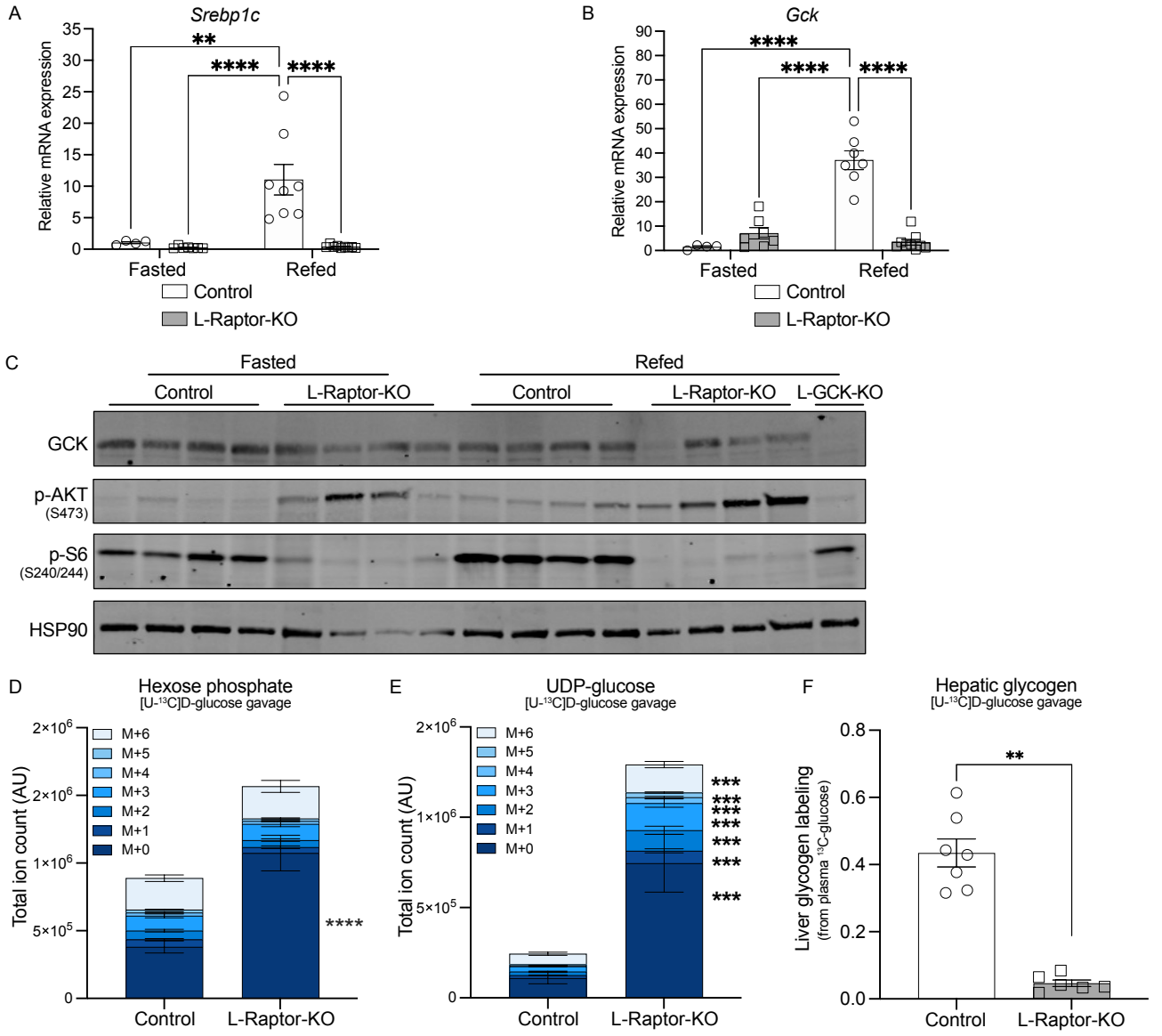

Figure 2: mTORC1 is required for hepatic glycogen synthesis
(A) 10-12 week old *Rptor*$^{loxP/loxP}$ or *Gck*$^{loxP/loxP}$ mice were injected with AAV-TBG-GFP (Control) or AAV-TBG-Cre (L-Raptor-KO or L-GCK-KO). (A,B) 2 weeks after AAV injection, mice were fasted overnight and refed for 4 hours before sacrifice. (A,B) Gene expression of Srebp1c and Gck (glucokinase). (C) Immunoblot of glucokinase (GCK) protein, activation of AKT, and inhibition of mTORC1 signaling. (D-F) 2 weeks after AAV injection, mice were fasted overnight and subjected to oral gavage with 2g/kg U-13C-D-glucose. Mice were sacrificed and livers were harvested 30 minutes after oral gavage. (D,E) Total ion count of hexose phosphate and UDP-glucose and respective mass isotopomer distribution in liver tissue. (F) Hepatic glycogen labeling representing the average carbon labeling enrichment of glycogen from oral gavage of [U-13C]-glucose normalized to plasma glucose labeling (Supplemental Figure 2A,B). **p<0.01 vs control mice, ****p<0.0001 vs control fed mice via 2-way ANOVA (A,B) or students t-test (D-F). Data show in in +/- SEM.

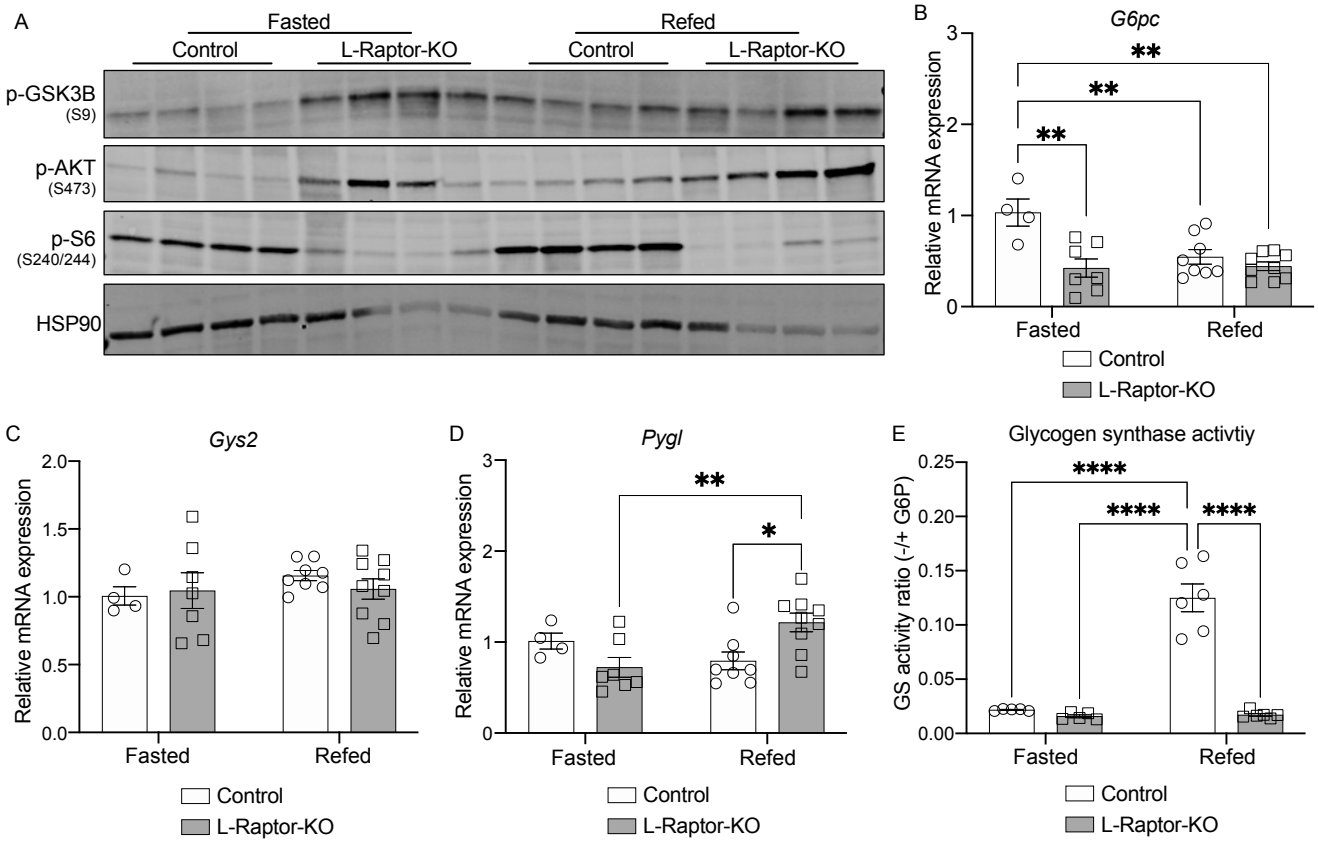

Figure 3: mTORC1 controls glycogenesis through regulation of GS activity
(A-E) 10-12 week old *Rptor*$^{loxP/loxP}$ mice were injected with AAV8-TBG-Cre (L-Raptor-KO) or AAV8-TBG-GFP (Control). 2 weeks after injection, mice were fasted overnight (Fasted), or refed for 4 hours (Refed) before sacrifice. (A) Immunoblot of lysates from refed livers. (B-D) Relative mRNA expression of *G6pc* (glucose-6-phosphatase), *Gys2* (glycogen synthase), and *Pygl* (glycogen phosphorylase), respectively. (E) Glycogen synthase (GS) activity measured as a ratio in the presence or absence of saturated glucose-6-phosphate. **p<0.01, ***p<0.001, ****p<0.0001, via 2-way ANOVA. Data shown in +/- SEM.

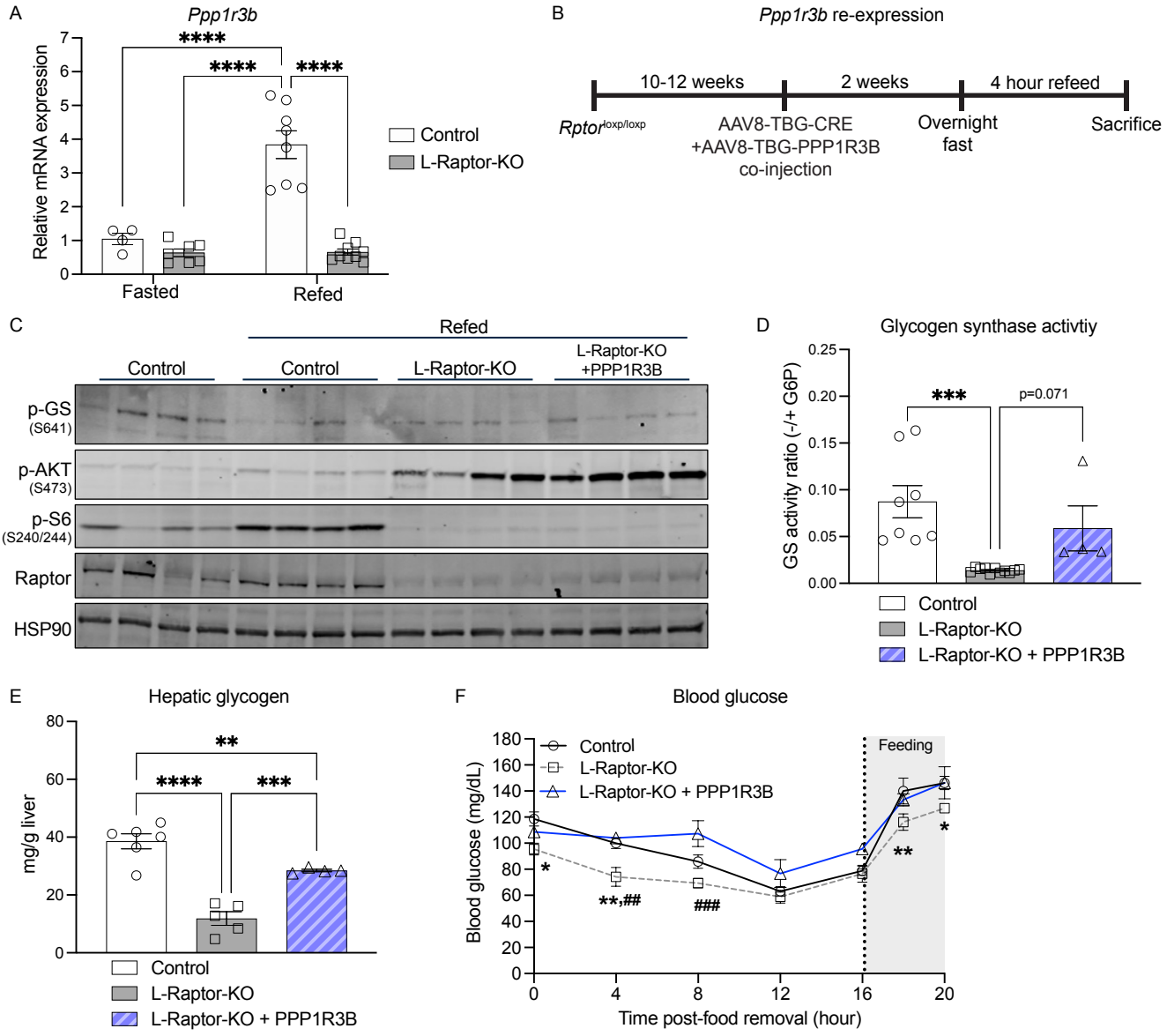

Figure 4: Restoration of *Ppp1r3b* in L-Raptor-KO livers promotes GS activity and glycogen storage
10-12 week old *Rptor*$^{loxP/loxP}$ mice were injected with AAV8-TBG-GFP (Control), AAV8-TBG-Cre in combination with AAV8-TBG-GFP (L-Raptor-KO), or AAV8-TBG-Cre in combination with AAV8-TBG-Ppp1r3b (L-Raptor-KO + Ppp1r3b), two weeks prior to an overnight fast and 4 hour refed. (A) Relative mRNA expression of *Ppp1r3b*. (B) Experimental schematic. (C) Immunoblot of liver lysate, indicating inhibition of mTORC1 signaling following co-injections of AAV, and changes in phosphorylation of glycogen synthase (GS). (D) Glycogen synthase (GS) activity measured as a ratio in the presence or absence of saturated glucose-6-phosphate in refed livers. (E) Hepatic glycogen measured in fed livers. (F) Blood glucose measurement at indicated time following food removal. At hour 16, mice were given food, as indicated by "feeding" notation for gray area. *p<0.05, **p<0.01, ***p<0.001, ****p<0.0001 vs. indicated genotype via 2-way ANOVA (A) or one-way ANOVA (D-F). Data shown in +/- SEM.

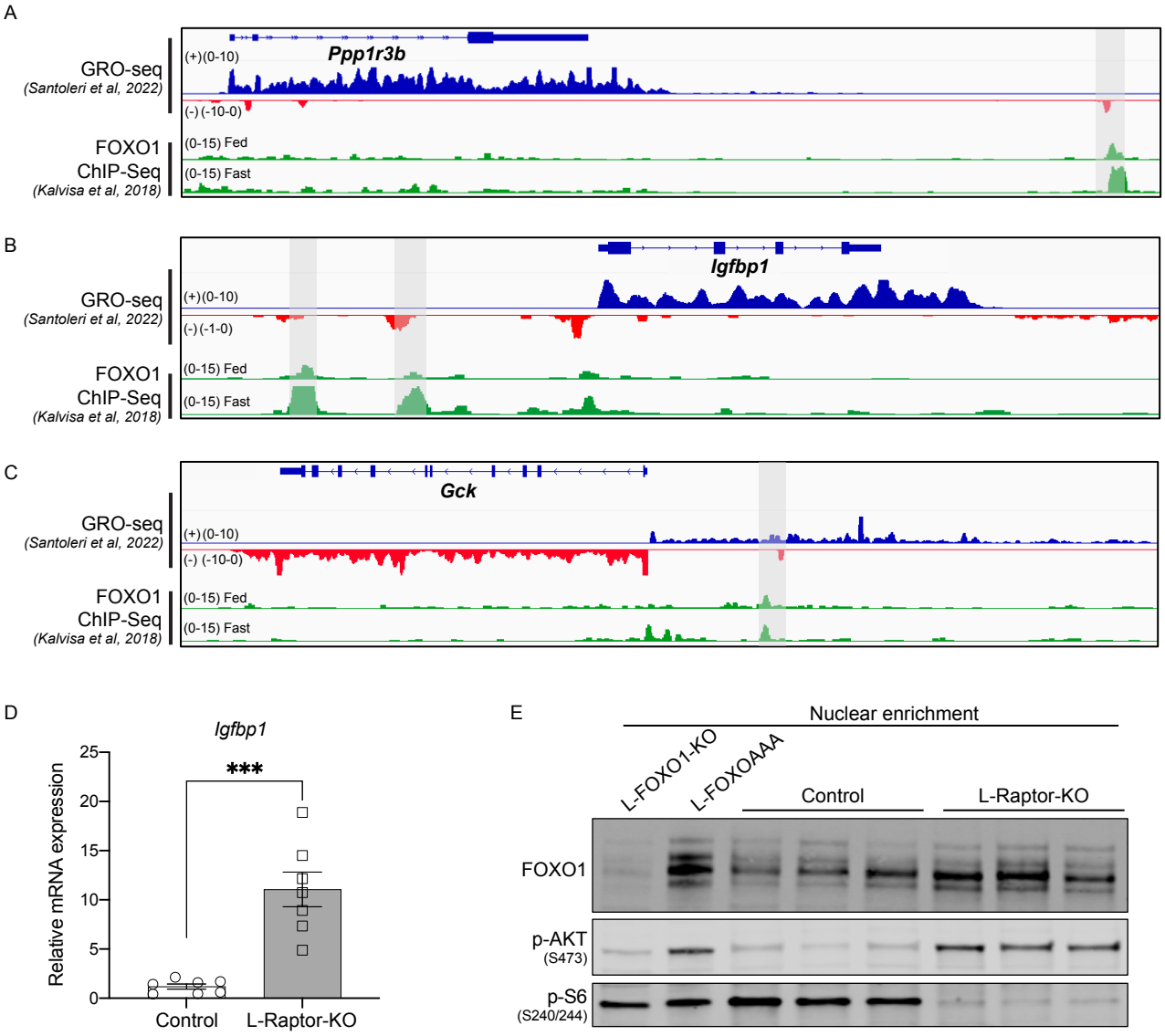

Figure 5: mTORC1 activity is required for AKT-mediated inhibition of FOXO1
(A-C) Genome browser track (mm9) GRO-seq displaying Ppp1r3b and nearby eRNA corresponding with a FOXO1 ChIP-seq track with previously identified FOXO1 binding highlighted in grey near genes (A) *Ppp1r3b*, (B) *Igfbp1*, and (C) *Gck*. (B) mRNA expression of *Igfbp1* in refed L-Raptor-KO livers. (C) Immunoblot of FOXO1 from refed liver lysates of Control, L-Raptor-KO, L-FOXO1-KO, and L-FOXOAAA enriched for nuclear fraction. ***p<0.001 vs. \ control via students t-test. Data shown in +/- SEM.

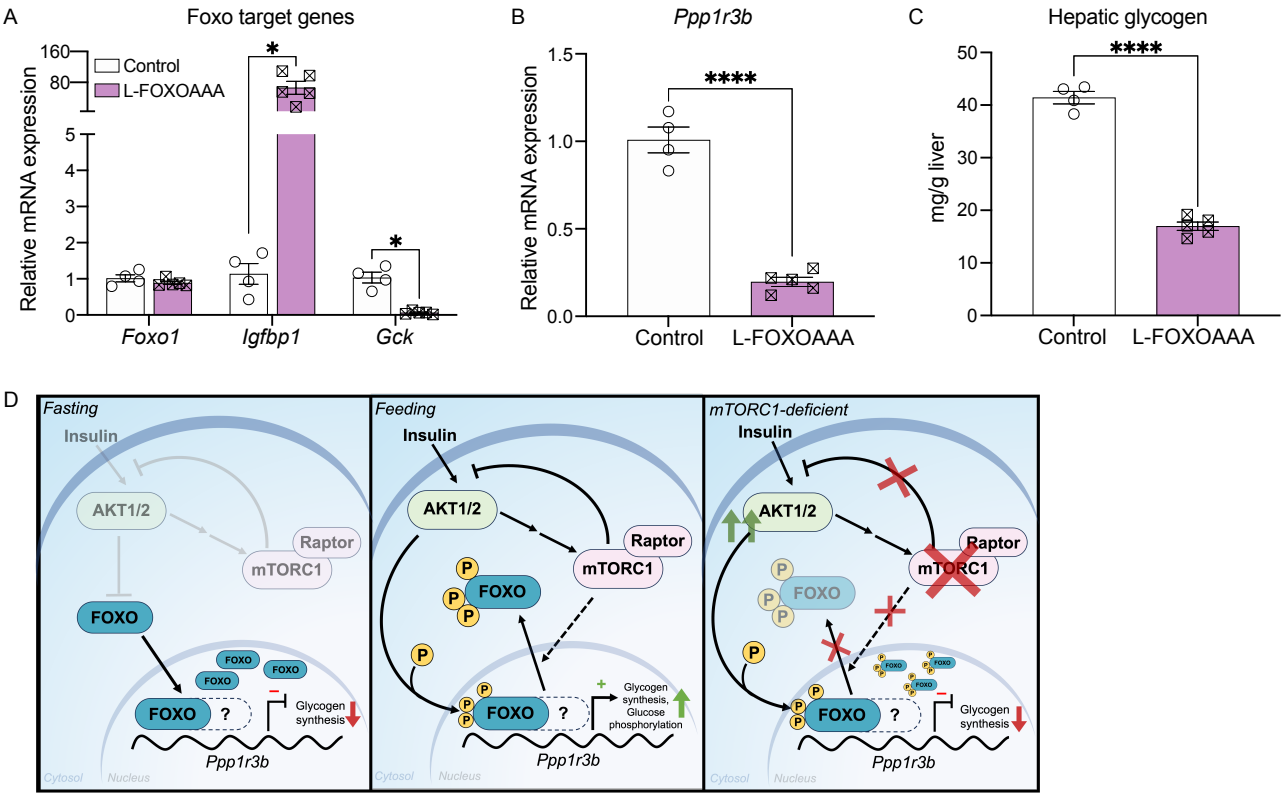

Figure 6: Activation of FOXO1 is required for *Ppp1r3b* repression
10-12 week old Foxo1^{AAA} mice were injected with AAV8-TBG-Cre (L-FOXOAAA) or AAV8-TBG-GFP (Control). Two weeks after injection, mice were fasted overnight, then refed chow for 4 hours before sacrifice. (A) Relative mRNA expression of FOXO target genes. (B) Relative mRNA expression of *Ppp1r3b*. (C) Hepatic glycogen levels in refed livers. (D) Mechanistic schematic. Under fasting conditions, AKT and mTORC1 are inhibited, FOXO localizes to the nucleus where it recruits an unidentified co-repressor (vvrepresented by the dashed line and '?') to suppress transcription of Ppp1r3b, along with repression of Gck, to downregulate glycogen synthesis. Under feeding conditions, AKT facilitates phosphorylation of FOXO proteins and mTORC1 promotes the nuclear exclusion of AKT-phosphorylated FOXO (unknown mechanism represented by dashed arrow) to inhibit FOXO and promote transcription of *Ppp1r3b* and *Gck*. In the absence of mTORC1, AKT-phosphorylated FOXO proteins remain localized in the nucleus and continue to repress Ppp1r3b and Gck. *p<0.05, ****p<0.0001 vs. indicated control via students t-test. Data shown in +/- SEM.